

Contract No.:

This manuscript has been authored by Battelle Savannah River Alliance (BSRA), LLC under Contract No. 89303321CEM000080 with the U.S. Department of Energy (DOE) Office of Environmental Management (EM).

Disclaimer:

The United States Government retains and the publisher, by accepting this article for publication, acknowledges that the United States Government retains a non-exclusive, paid-up, irrevocable, worldwide license to publish or reproduce the published form of this work, or allow others to do so, for United States Government purposes.

Comparing and Contrasting In-Vial and Full-Scale Systems for Sparging Volatile Analytes

Brian B. Looney^{a*}, Holly H. Vermeulen^{ab}, Andrew J. Boggess^{ac}

^a Savannah River National Laboratory, Savannah River Site, SC, USA 29808

* Corresponding author: SRNL Earth and Biological Systems, 773-42A, Aiken, SC, USA 29808;

1(803)507-4425; brian02.looney@srnl.doe.gov

^b holly.vermeulen@srnl.doe.gov

^candrew.boggess@srnl.doe.gov

Abstract

In-vial sparging was demonstrated as an effective, practical alternative to a full-scale sparging system for supporting the analysis of volatile constituents. Using elemental mercury (Hg^0) and toluene as representative purgeable analytes, the mass removal for various sparge configurations was measured and a reduced order model was developed and validated. In the primary experiments, Hg^0 in the sparge gas was trapped on activated carbon or gold, thermally desorbed, and quantified using atomic absorption or atomic fluorescence spectroscopy. Toluene experiments using the same in-vial sparge apparatus and sparge parameters were performed to demonstrate the applicability of the reduced order model to a broad range of compounds. Toluene removal was tracked by measuring the remaining toluene in sparged aliquots using Ultraviolet-visible (UV-Vis) spectroscopy. For the sparging, flow rates varied from 25 to 75 mL/min for periods from 0 to 30 minutes. Sparge performance, mass removal as a function of time, and sparge gas volume were measured for both in-vial and full-scale systems. A model based on dimensionless Henry's Law coefficient, normalized sparge gas volume, and fractional extent of equilibrium matched the experimental data for both compounds and provides a practical tool for future applications. For the conditions tested in this study, the calibrated model indicated that the sparge gas in the in-vial system reached approximately 33% of its equilibrium value before exiting the water surface, while a full-scale system reached approximately 100%. The tests validated the quality, reproducibility, and predictability of sparging performance for both full scale and in-vial sparge systems. Related factors such as waste generation, worker risk, and labor were also assessed. Full scale sparge systems provide the advantage of lower detection levels due to larger sample volume, while the in-vial sparge systems provide advantages for most other factors; including automatability, reducing secondary wastes, lessening the need to clean and check the sparge apparatus, and lowering labor and costs. The data and associated reduced order model support continued development and deployment of in-vial sparge platforms as a practical option for analysis of purgeable analytes such as volatile organic compounds and volatile metals/organometallics.

Keywords

purge-and-trap, sparging, headspace methods, mercury, volatile organic compounds

1. Introduction

Standard analytical methods for volatile or semivolatile analytes often rely on sparging target compounds from aqueous solution into a gas phase. For inherently purgeable constituents such as volatile organic compounds (VOCs) or elemental mercury (Hg^0), standard purge-and-trap protocols and other dynamic headspace methods directly remove the constituents from the solution via sparging. Applications of sparging methods to other analytes rely on selective reduction, oxidation, or derivatization to generate a purgeable species. Once the target analytes are sparged from solution, the flowing gas is directed to an appropriate downstream analysis schema, detector, or instrument. Many protocols maximize performance by concentrating the analytes on a trap. The concentrated material is then thermally desorbed as a sharp peak into a detector or an instrument, such as a gas chromatograph (GC), for quantification.

Notable examples of a protocols that rely on purging from aqueous solution are those for the analysis of mercury for total and various mercury species in water samples (Environmental Protection Agency (EPA) Methods 245.1, 245.7, 1630 and 1631) [1, 2, 3, 4]. These protocols rely on room temperature chemical conversion of target aqueous phase mercury species into volatile forms of mercury, including chemical reduction of ionic mercury to Hg^0 , or derivatization of mono-substituted organo-mercury ions to fully substituted volatile forms such as methyl ethyl (or methyl propyl) mercury. Following the reactions, the mercury is purged into a trap or into an instrument or detector. Techniques commonly used for detection and quantification of the purged mercury include atomic fluorescence spectrometry (AFS), atomic absorbance spectrometry (AAS), Zeeman effect spectroscopy (ZES), or mass spectroscopy (MS). Any of these detectors can be preceded by GC to separate various gas phase mercury compounds. EPA Method 1630, for example, is the baseline approach for measuring organomercury. Additional speciation information can be obtained by direct purging of a sample with no reagents or selective

reduction/derivatization followed by subsequent purging. For VOCs, purged constituents are typically collected in a downstream trap and thermally desorbed into a GC for separation with quantification using MS or similar detector (EPA Method 524.3 [5]).

Full-scale sparging traditionally employs relatively large (e.g., 200 mL) vessels, uses large volumes of liquid sample and sparge gas, and provides for effective mass transfer and long residence times. The goal of the standard full-scale design is to optimize sparging effectiveness and maximize total collected analyte mass. These full-scale systems are designed for complete transfer of volatile analytes into the gas phase. A typical full-scale sparge apparatus is depicted in Figure 1a. Full-size systems require significant sample handling and are difficult and labor intensive to operate and clean. Large volumes of sample are used and large volumes of acidic or solvent waste are generated during the cleaning process. Significant labor is required for system assembly and to assure effective cleaning to avoid carryover. Techniques that mitigate or minimize these various challenges are actively being developed and adopted by researchers, instrument manufacturers, and commercial laboratories.

A number of detailed, mechanistic models exist that describe the dynamic sparge process based on detailed constitutive relationships [6, 7, 8, 9, 10]. Boggess et al. [11] reports an increase in sparging extent with an increased purge flow rate and total gas volume; consistent with maintaining equilibrium partitioning between sparge gas and solution in an optimized sparge apparatus. The design of systems employed during sparging affect the size and size distribution of bubbles generated and the gas liquid contact time, which ultimately impact the effectiveness of the mass transfer [6]. Factors like injection pressure and injection orifice size influence the size and size distribution of the bubbles generated during sparging and a nonuniform bubble distribution contributes to a reduction in sparging efficiency [6]. Bubble size variation has an impact on mass transfer and affects the overall rate of reaction [8]. An increase or decrease in bubble surface area with size determines the mass transfer rate at the gas-liquid interface. Many of these models also utilize bubble size in overall rate of absorption estimations. In general, adsorption of a gas occurs as a function of bubble diameter and the contact time of the bubble, which is determined by the water column height and rate of ascension of that bubble to the water-air interface [7]. These parameters have been quantitatively demonstrated to impact the behavior of purgeable constituents [10]. Adsorption of compounds to the bubble surfaces, influenced by matrix (e.g., surfactants or oils), temperature, and compound chemistry, can cause excess or deficient capture by the gas phase and, consequently, disequilibrium with simple partitioning models [9]. In practice, it is often challenging to quantify key parameters in the detailed constitutive models and to separate effects of matrix, physical, and chemical factors in these complex dynamic systems.

Alternative equilibrium-based models have also been developed to describe the performance of headspace methods such as those used for purge and trap protocols. Novak [12] and others [13, 14, 15, 16, 17, 18, 19, 20] describe simplified models for dynamic headspace methods. These models use the bulk distribution coefficient of constituents between phases to predict the progressive stripping of solutes into the gas phase. Such mathematical constructs overcome the complexities of the constitutive models, but these methods generally assume that the gas reaches equilibrium with the solution. Extensive scientific literature, such as those references cited above, demonstrate that optimized systems, such as a full scale sparge apparatus or specially designed sparge tubes, are relatively effective at partitioning constituents into the gas phase and have generally conformed to the performance predictions and the presumption of equilibrium in this class of model.

Recently, simpler in-vial sparge systems and modular concentrator units that use small (e.g., 5 mL to 15mL) subsamples are emerging as practical alternatives to the full-scale design. In-vial sparge and aliquot-based systems (e.g., Figure 1b) offer several advantages over traditional full-scale systems for analysis of purgeable constituents such as Hg⁰ and VOCs. However, scientific literature, data and publications quantitatively comparing the performance of the full-size standard sparge system and smaller scale sparge systems is limited. In-vial and aliquot-based sparge systems are generally simpler to operate.

These systems employ smaller volumes and often shorter sparge times for both samples and standards. Typical systems use disposable vials, eliminating the labor and wastes associated with cleaning reusable glassware. The smaller sample volumes and disposable vials result in reductions in waste generation. In most commercial applications, purge times are standardized, resulting in the presumed sparging of a consistent fraction of target volatile analytes. A key advantage of the in-vial sparge and aliquot-based systems is that these can be automated to provide reproducibility in flow rate and sparge time and provide capabilities for pre-staging multiple samples for unattended operation. A key disadvantage of the in-vial sparge system is that the small sample vials are not optimally configured for sparging. Bubbles produced by the typical needle assembly are often larger than those generated by a diffuser and the bubble residence time in solution is limited due to the small sample volume and limited liquid-gas contact distance and time. While use of short, consistent sparge times and volumes provides an effective method for generating a reproducible standard curve, high-quality data, and rapid throughput, sparge times of only a few minutes in an unoptimized configuration are inadequate to completely sparge analytes from aqueous samples [13, 21]. In most cases, the sparge time and flowrates are set based on general guidelines and experience.

Additional quantitative data are needed to document the relative performance of full scale and in-vial, or aliquot-based, sparge systems and to provide additional technical basis for selecting the optimal sparge apparatus and/or conditions for a variety of scenarios. By using high quality analytical standards, the following experiments using Hg^0 and toluene as a surrogates provide a simple and straightforward basis for generating comparative data and developing a straightforward, practical model.

In this research, measured performance data for in vial sparging and for full scale sparging were used to formulate and demonstrate a reduced order mathematical model. The proposed model is an extension of the equilibrium-based Novak [12] and successor models, modified to support application to systems that do not reach equilibrium. The objective of the reduced order model was to match and quantitatively predict relative sparging effectiveness and sparge progress for the in-vial sparge system and the standard full-scale sparge system. As shown in Figure 1c, the reduced order model utilizes dimensionless Henry's Law coefficient (H_{cc}) to describe the dynamic partitioning of volatile constituents, in this case Hg^0 and toluene into the sparge gas. An exponential equation describes sparging progress based on a mass balance in a completely stirred tank reactor, equilibrium-based partitioning into the gas phase, and integration over time [13]. If the sparge gas reaches H_{cc} equilibrium before exiting the solution, then the resulting model predicts the normalized purge performance of an optimized sparger as a simple function of H_{cc} and the air: water ratio, β . The model for this optimized case is identical to Novak [12] and similar models. For predicting in vial sparge performance in cases where the gas does not reach equilibrium, the model was extended to include a factor (ξ) describing the extent of reaction in terms of fractional progress of the partitioning toward complete equilibrium. The resulting model, based on easily measured emergent data, provides a simpler alternative to the constitutive-mechanistic models currently in the literature and expands capabilities to predict non-optimized systems compared to equilibrium models. Since the proposed exponential model reduces the need for detailed information on parameters that are difficult to measure, it provides a tool that may be more practical for understanding the relative performance of alternative sparge configurations compared to a baseline optimized sparge apparatus, as well as support scoping, developing, designing, and validating diverse analytical protocols.

2. Material and methods

2.0. Reagents and Equipment

Full details of the analytical protocols, reagents, instruments, and settings used for analysis of both mercury and toluene are provided in the supplementary materials.

The mercury testing used certified inorganic mercury standards (High Purity Standards and Brooks-Rand Instruments) and a reducing stannous chloride reagent prepared according to [3] from ACS reagent grade

stannous chloride and hydrochloric acid (Fisher Scientific) to generate known quantities of Hg^0 in each vial. The mass of mercury in the gas sparged through each apparatus or vial was collected in traps packed with gold coated sand or with high surface area activated carbon beads. A confirmatory evaluation was performed using the in-vial sparge system with toluene (Fisher Scientific) solutions. The objective of the confirmatory evaluation was to determine if a robustness of the reduced order model, Table 1 summarizes relevant physical and chemical properties for the two tested analytes. Modeling predictions that effectively match the sparge behaviors for these two disparate compounds (a volatile metal and a VOC which have substantially different diffusion coefficients in water & air, aqueous solubilities, vapor pressures, octanol water partition coefficients, boiling points, melting points and related properties) supports the potential for a general ability of the reduced order model to inform experimental designs and to provide predictions for a range of purgeable constituents.

2.1. Sparge model

The sparge performance data was used to formulate and inform a mathematical model to predict sparging effectiveness of the in-vial sparge system and the standard full-scale sparge system. The sparge model is an extension of the simple analytical solution described by Looney et al. [13] in which a volatile analyte, such as gaseous Hg^0 or toluene, partitions into the sparge gas according to a H_{cc} :

$$H_{cc} = \frac{\left(\text{concentration of } Hg^0 \text{ in gas phase in consistent units such as } \frac{ng}{mL}\right)}{\left(\text{concentration of } Hg^0 \text{ in liquid phase in consistent units such as } \frac{ng}{mL}\right)} = \frac{[Hg^0]_{gas}}{[Hg^0]_{liq}} \quad (1)$$

H_{cc} is a conditional parameter that can vary if the solution matrix changes significantly. However, for volatile constituents that are not subject to confounding solution reactions, this parameter has proven to be robust and broadly useful in environmental chemistry applications. In matrices associated with environmental samples, H_{cc} values for most constituents are well documented, relatively stable, and consistent. H_{cc} values for most volatile constituents are reported in the literature and are tabulated in widely available databases such as in the US EPA Estimation Program Interface (EPI) Suite [23]. The literature often provides information on H_{cc} as a function of temperature and other key solution factors, providing the basis for broad use of a H_{cc} based model formulation for understanding and scoping sparging performance for analytical methods. As shown in Table 1, the estimated H_{cc} for Hg^0 at 20 °C is approximately 0.305 and the estimated H_{cc} for toluene is approximately 0.195.

In an optimized configuration, the sparge system is treated mathematically as a completely stirred reactor and the sparge gas is assumed to reach equilibrium with the contacted liquid. Mercury is removed from the liquid over time, resulting in an exponential equation describing sparge progress [13]. Based on mass balance and integration over time, the normalized purge performance of an optimized sparger can be fully approximated as a simple function of H_{cc} and the air: water ratio, β :

β = the ratio of the purge air volume to the fixed water volume in the vessel using consistent units

$$= \frac{(\text{gas flow rate in std mL per minute})(\text{purge time in minutes})}{(\text{liquid volume in purge vial in mL})} \quad (2)$$

We extended the analytical solution from Looney et al. [13] to assess the relative performance of an in-vial sparge system by assuming that the incoming sparge gas may not achieve complete equilibrium and by including a term (ξ , ranging from 0 to 1) that represents how much progress is made toward equilibrium in the gas bubbles before they exit the liquid surface. The metric for sparge progress is the normalized mass removal from the starting solution in the sparger. The resulting modified analytical solution is:

$$\text{normalized fraction of mass removed as a function } \beta \text{ and } \xi = \frac{M_{(\beta)}}{M_{(0)}}$$

$$= 1 - e^{-\xi H_{cc}\beta} \quad (3)$$

where $M_{(0)}$ and $M_{(\beta)}$ are the initial mass and remaining mass as a function of sparge progress, respectively.

At any stage of the sparge process, $M_{(\beta)}$ is equivalent to solution concentration multiplied by the volume of liquid in the sparge apparatus. In an optimized sparge system, $\xi = 1$ and the resulting equation simplifies to a form that is analogous to that reported by Novak [12], Looney et al. [13], and others. The measured performance of in-vial sparge systems will support generating ξ values that will facilitate technically based deployment of small scale in-vial sparge and modular configurations.

2.2. Sparge tests

Hg^0 was used for method development since the H_{cc} for Hg^0 is well documented and this constituent can be quantitatively generated in aqueous solution using high-quality inorganic mercury analytical standards and stannous chloride reductant. The in-vial sparge system vials were loaded with 15 mL of liquid and gas flow rates for the in-vial sparging ranged from 50 to 75 standard mL/min for periods from 0 to 13 minutes. The confirmatory in-vial sparge testing using toluene was performed on the same test stand using equivalent conditions – 40 mL vials containing 15 mL of aqueous sample and a sparge gas flow rate of 75 standard mL/min, and sparge times ranging from 0 to 10 minutes. The full scale sparge systems were loaded with 100 mL of liquid and sparge gas flow rates in the full scale sparge tests ranged from 25 to 65 standard mL/min for periods from 0 to 30 minutes.

The full scale sparging and analysis were performed using EPA Method 245.7 using standard sparging glassware, and modular units for flow control, amalgamation onto gold coated sand, thermal desorption and AFS (Brooks-Rand Instruments) (Figure 1a). The in-vial sparging and analysis were performed using EPA Method 7473 using a manual in-vial sparging test stand (Tekran Instruments) (Figure 1b). The in-vial and full-scale mercury analysis methods have been previously documented and validated [11, 21, 22].

A custom Ultraviolet (UV) spectroscopy method was developed for analysis of toluene to allow experimental testing in the same sparge apparatus under the same conditions of sample volume, flow, and needle assembly. A toluene stock solution prepared from ACS reagent grade toluene (Fisher Scientific) was added to each test vial prior to sealing and testing. Upon completion of sparging, liquid samples were collected, placed in sealed quartz cuvettes with no headspace, and analyzed within ten minutes of collection using a Thermo Scientific Genesys 10S Ultraviolet-visible (UV-Vis) spectrometer. This method provided quantitative data on the residual toluene in the sparged solution and supported calculation of the sparge progress for varying sparge times and sparge gas volumes. Additional details on the sparging systems and the analytical protocols for both mercury and toluene are provided in the supplementary material.

2.3. Model validation

The data from the in-vial sparge system method development study was used to determine the ability of the proposed reduced order analytical model to match the progress of sparging for the test compounds and conditions and statistically assess the quality of the model predictions. Several quantitative metrics for model prediction were calculated, a bivariate correlation of paired data, measured and predicted, using Pearson product-moment correlation coefficients (Pearson r), a calculated bias for each data pair, and an average bias. The Pearson r and average bias metrics were calculated for the entire dataset and for the various data subsets.

3. Results and Discussion

3.1. Sparge tests

As shown in the primary set of experiments using vapor-phase Hg^0 , sparging results for the in-vial sparge apparatus and full scale sparge apparatus (Figure 2), demonstrated steadily increasing sparge progress until the mass was depleted, as well as complete and quantitative recovery of the spiked mercury for

samples with long sparge times (high air-water ratio). The accuracy and precision of the mercury data were within the documented instrument performance specifications ($2\sigma \cong 15\%$) and no mercury breakthrough was observed onto the backup traps (see supplemental information). For mercury, the data confirm accurate spiking, complete conversion of the inorganic ionic mercury in solution to volatile Hg^0 , effective sparging at later times, and complete capture of the sparged Hg^0 by gold trap (for the full-scale tests) and activated carbon traps (for the in-vial testing). In the mercury tests, the in-vial sparging lagged the full scale sparging as a function of air: water ratio. This relative performance is consistent with the expectation of a higher sparge effectiveness in the optimized full scale apparatus design.

Figure 3 depicts the comparative data for the in-vial testing for both mercury and toluene. The general behavior of the data for toluene is similar to the general behavior of mercury; notable, steadily increasing sparge progress until the mass was depleted, as well as complete and quantitative recovery of the spiked toluene for samples with long sparge times (high air-water ratio). In these tests toluene sparging lagged Hg^0 sparging as a function of air: water ratio. This relative performance is consistent with the partitioning properties of test analytes. Toluene has a lower H_{cc} than Hg^0 .

3.2. Model validation

In Figure 2, the theoretical reduced-order model predictions for Hg^0 sparging performance in an optimized system with a ξ of 1.0 is plotted for comparison, along with measured data generated using standard full-size sparge equipment. This comparison data was previously documented in the literature [e.g., 13, 21] and assumes the sparge gas reaches 100% of its theoretical equilibrium value. The standard-full-size sparge system provided effective and complete mass transfer and the data closely match the theoretical prediction. Similarly, for the in-vial sparge system, the reduced order model prediction for Hg^0 closely matches the data using a best fit ξ of 0.33. According to the data and model, the full-scale sparge system completely purges Hg^0 at air: water ratios greater than approximately 15, while the small in-vial sparge system purges all of the Hg^0 at air: water ratios greater than approximately 40. This difference may be less significant in practice, however, because the full-size system uses larger volume samples that have often been diluted; thus, increasing the required purge gas volume and time.

Data from the in-vial sparge system for the two test compounds are depicted in Figure 3. The general shape of the model fit and each individual model prediction for both compounds closely match the measured data for a consistent ξ value of 0.33. This value was developed based on fitting the initial mercury experiments and using the Table 1 unmodified literature reference values for H_{cc} . This suggests that the purge gas in the in-vial system reached approximately 33% of its theoretical equilibrium value before exiting the liquid surface for the conditions of the testing and for both tested compounds. The general match for both compounds using a single ξ value supports the robustness of the proposed model. For commercial laboratories using the in-vial sparge apparatus, a short sparge time is often used to increase throughput. A 3-minute sparge time (equivalent to an air: water ratio of 10) would reproducibly purge a constant amount, approximately 78%, of the Hg^0 from each sample/standard in dilute aqueous solutions and approximately 55% of toluene from dilute aqueous solutions.

A key assumption and conceptualization related to the robustness of the reduced-order model is that the ξ value is primarily influenced by system components and operations. Thus the ξ for any sparge system will be most sensitive to a) sparge needle or diffuser design and the associated gas bubble size distribution, b) the sparge vessel geometry and volume of water and the associated water column height for bubble exposure, and c) other operational conditions that directly influence equilibrium partitioning such as temperature. According to this conceptualization, the influence of some of the compound specific parameters that underpin many constitutive models, such as gas and liquid phase diffusion coefficients, would, have a lesser practical impact on the model predictions. Thus, to adequately verify the reduced-order model, the model predictions need to be accurate for disparate compounds (e.g., both Hg^0 and

toluene) using the same ξ . The key assumptions are supported if a single ξ value provides effective predictions for both compounds.

A bivariate correlation of paired data, measured and predicted, was performed. Five Pearson r correlation coefficients were calculated for the validation: 1) an overall correlation for all conditions and both compounds, 2) three correlation coefficients for the mercury only tests (overall, full scale, and in vial), and 3) a correlation coefficient for the toluene only in-vial test. A strong positive correlation for the overall data supports the constitutive formulation of the model as technically reasonable. Strong correlations with similar absolute magnitudes for the overall dataset, the mercury-only datasets and toluene-only dataset support the robustness of the reduced order model to predict sparge performance for compounds with substantively different chemical and physical properties.

Figure 4 depicts the graphical relationship of the bivariate paired data for all compounds and conditions. This figure includes the full scale and in-vial results for mercury and the in-vial results for toluene. For the entire dataset shown in Figure 4, the Pearson r was 0.999 and the average estimation bias was + 0.014. The span of the normalized data was 0 and 1, and the individual bias calculations indicate that the model prediction was typically within a + 0 to 3% of the measured data.

The quantitative fit relationships for the various data subsets were similar to the overall dataset. The separate detail graphs of the correlations for the various subsets of data are provided in the supplementary material and are summarized below. The Pearson r and average bias for the overall mercury data set was 0.999 and + 0.012, respectively. For the in-vial sparge mercury dataset, the Pearson r and average bias were 0.998 and + 0.004, respectively. For the full-scale mercury dataset, the Pearson r and average bias were 0.999 and + 0.018, respectively. For the in-vial toluene dataset, the Pearson r and average bias were 0.996 and + 0.021, respectively. The entire dataset and all the various data subsets showed a high degree of correspondence between the measured values and the model predictions with the Pearson r for the paired measured data to the reduced order model predictions > 0.996.

4. Conclusions

The various tests confirmed and extended the information in the scientific literature. Laboratory data validated the quality, reproducibility, and predictability of the performance of a compact sparge configurations such as in-vial sparge systems and aliquot-based sparge systems. A reduced order analytical model based on two parameters, Henry's Law partitioning and normalized sparge volume, matched the data generated by both in-vial and full-scale sparge systems for both Hg^0 , a purgeable metal, and toluene, a purgeable VOC. For the specific in-vial apparatus and conditions tested, the calibrated model indicated that the sparge gas reached approximately 33% of its equilibrium value before exiting the water surface for both tested compounds. The full scale sparge apparatus, consistent with its design basis (small bubble size and long contact time), was well predicted by the theoretical case where the sparge gas reaches 100% of its equilibrium value.

Related factors such as waste generation, worker risk, and labor also impact the viability and practicality of alternative sparge platforms. Full scale sparge systems provide the advantage of lower detection levels due to larger sample volumes, while the in-vial sparge systems provide advantages for most other factors such as reducing secondary wastes, lessening the need to clean and check the sparge apparatus, automatability, and lowering labor and costs.

The proposed reduced-order model focuses on emergent system behaviors and does not provide an *a-priori* prediction of ξ . Instead, the model must be calibrated to determine a conditional ξ by collecting representative information using one or more compounds of known H_{cc} . Further, the proposed model assumes a dilute-simple matrix or, alternatively, a consistent matrix for calibrating ξ and then for running samples. The model assumes low or consistent levels of the following: surfactants, competing phases such as sorbents or separate phase organics, ionic strength, and other solutes/conditions that can complex

or otherwise react with target analytes in solution. Note that these cautions are not unique to the proposed model, but they universally apply for reliable purge and trap and similar sparge-based analytical methods. The proposed model is applicable to purgeable analytes that are volatile or semivolatile analytes and which have low to moderate solubility that are amenable to purging.

The equilibrium-based mass balance model was demonstrated as a practical tool to facilitate designing and deploying sparge or purge-and-trap methods. Initially, the ξ for any subject dynamic headspace configuration (in vial or aliquot-based using a specific liquid volume) can be estimated by measuring sparge progress as a function of air water ratio for a constituent that has a known H_{cc} . The best sparge conditions (flow rate and time) for applying the method to multiple constituents can then be developed based on the resulting estimated ξ , along with the H_{cc} of the least volatile target analyte, assuring the effectiveness post sparge traps to avoid breakthrough, and evaluating the appropriate balance of throughput and robustness. Higher air: water ratios increase sensitivity and reduce analytical variability because the mass removal increases, and the mass removal curve flattens as β increases. For any purgeable constituent, the model provides an estimate of the β needed for complete sparging to support mass balance calculations and provide a tool for cross checking and enhancing quality assurance. Alternatively, if short analysis times and high throughput are primary drivers in a method deployment for samples with consistent bulk matrices, then the model would support implementing sparge times that would provide a desired level of sparging to reproducibly achieve target detection levels. The model also supports use of previously calibrated in-vial sparging systems to determine conditional H_{cc} values for compounds where such data are not available in the literature. The results from this research and the associated reduced order model support continued development and deployment of in-vial and aliquot-based sparge platforms for analysis of purgeable analytes such as various mercury species, other volatile metals-organometallics, and VOCs. The results demonstrate that these sparge systems are practical, and possibly preferred, alternatives in appropriate laboratory scenarios.

References

- [1] U.S. EPA, Method 245.1, Determination of mercury in wastewater by cold vapor atomic absorption spectrometry, Revision 3.0, U.S. Environmental Protection Agency Office of Research and Development Environmental Systems Monitoring Laboratory, Cincinnati OH (1994) 188. <https://www.epa.gov/sites/default/files/2015-06/documents/epa-245.1.pdf>.
- [2] U.S. EPA, Method 245.7, Mercury in water by cold vapor atomic fluorescence spectrometry, Revision 2.0. EPA-821-R-05-001, U.S. Environmental Protection Agency Office of Water and Office of Science & Technology, Washington, DC (2005) 33. https://www.epa.gov/sites/default/files/2015-08/documents/method_245-7_rev_2_2005.pdf.
- [3] U.S. EPA, Method 1630 Methyl mercury in water by distillation, aqueous ethylation, purge and trap, and cold vapor atomic fluorescence spectrometry, U.S. Environmental Protection Agency Office of Water and Office of Science & Technology, Washington, DC (1998) 55. https://www.epa.gov/sites/default/files/2015-08/documents/method_1630_1998.pdf.
- [4] U.S. EPA, Method 1631, Revision E: Mercury in water by oxidation, purge and trap, and cold vapor atomic fluorescence spectrometry, EPA-821-R-02-019, U.S. Environmental Protection Agency Office of Water and Office of Science & Technology, Washington, DC (2002) 45. https://www.epa.gov/sites/default/files/2015-08/documents/method_1631e_2002.pdf.
- [5] U.S. EPA, Method 524.3, Measurement of purgeable organic compounds by capillary column gas chromatography / mass spectrometry, U.S. Environmental Protection Agency Office of Water and Drinking Water, Washington, DC (2009) 55.
- [6] S.E. Burns, M. Zhang, Effects of system parameters on the physical characteristics of bubbles produced through air sparging, Environ. Sci. Technol. 35 (2001) 204-208. <https://doi.org/10.1021/es001157u>.

- [7] F.H. Deindoerfer, A.E. Humphrey, Mass transfer from individual gas bubbles, *Fermentation Research and Engineering* 53 (9) (1961) 755-759. <https://doi.org/10.1021/ie50621a035>.
- [8] Kulkarni, Mass transfer in bubble column reactors: effect of bubble size distribution, *Ind. Eng. Chem. Res.* 46 (2007) 2205-2211. <https://doi.org/10.1021/ie061015u>.
- [9] Y.D. Lei, C. Shunthirasingham, F. Wania, Comparison of headspace and gas-stripping techniques for measuring the air-water partitioning of normal alkanols (C4 to C10): effect of temperature, chain length, and adsorption to the water surface, *J. Chem. Eng. Data* 52 (2007) 168-179. <https://doi.org/10.1021/je060344q>.
- [10] Shunthirasingham, X. Cao, Y.D. Lei, F. Wania, Large bubbles reduce the surface sorption artifact of the inert gas stripping method, *J. Chem. Eng. Data* 58 (2013) 792-797. <https://doi.org/10.1021/je301326t>.
- [11] A.J. Boggess, M.A. Jones, T.L. White, C.J. Bannochie, B.B. Looney, Selective capture and analysis of purgeable mercury species in high-activity tank waste at Savannah River Site, *Sep. Sci. Technol.* 54 (12) (2019) 1960-1969. <https://doi.org/10.1080/01496395.2019.1575420>.
- [12] J. Novak, *Quantitative Analysis by Gas Chromatography* (Chromatographic science; v. 5), Marcel Dekker, Inc, New York (1975), ISBN 0-8247-6311-4.
- [13] B.B. Looney, M.E. Denham, Jr., K.M. Vangelas, N.S. Bloom, Removal of mercury from low-concentration aqueous streams using chemical reduction and air stripping, *J. Environ. Eng.* (2003) 819-825. [https://doi.org/10.1061/\(ASCE\)0733-9372\(2003\)129:9\(819\)](https://doi.org/10.1061/(ASCE)0733-9372(2003)129:9(819)).
- [14] F. Ruiz-Beviaa, M. Fernandez-Torres, M. Blasco-Aleman, Purge efficiency in the determination of trihalomethanes in water by purge-and-trap gas chromatography, *Anal. Chim. Acta* 260 (632) (2009) 304-314. <https://doi.org/10.1016/j.aca.2008.11.022>.
- [15] J. Drozd, J. Novak, Quantitative head-space gas analysis by the standard additions method: Determination of hydrophilic solutes in equilibrated gas-aqueous liquid systems, *J. Chromatogr.* 136 (1) (1979) 23-36. [https://doi.org/10.1016/S0021-9673\(00\)82993-3](https://doi.org/10.1016/S0021-9673(00)82993-3).
- [16] E. R. Adlard, J. N. Davenport, A study of some of the parameters in purge and trap gas chromatography, *Chromatographia* 17 (1983) 421-425. <https://doi.org/10.1007/BF02262922>.
- [17] J. W. Graydon, K. Grob, F. Zuercher, W. Giger, Determination of highly volatile organic contaminants in water by the closed-loop gaseous stripping technique followed by thermal desorption of the activated carbon, *J. Chromatogr.* 285 (1984) 307-318. [https://doi.org/10.1016/S0021-9673\(01\)87772-4](https://doi.org/10.1016/S0021-9673(01)87772-4).
- [18] J. Curvers, Th. Noy, C. Cramers, J. Rijks, Possibilities and limitations of dynamic headspace sampling as a pre-concentration technique for trace analysis of organics by capillary gas chromatography, *J. Chromatogr.* 289 (1984) 171-182. [https://doi.org/10.1016/S0021-9673\(00\)95086-6](https://doi.org/10.1016/S0021-9673(00)95086-6).
- [19] Bianchi, M.S. Varney, J. Phillips, Modified analytical technique for the determination of trace organics in water using dynamic headspace and gas chromatography-mass spectrometry, *J. Chromatogr.* 467 (1989) 111-128. [https://doi.org/10.1016/S0021-9673\(01\)93956-1](https://doi.org/10.1016/S0021-9673(01)93956-1).
- [20] R. Kostianen, Effect of operating parameters in purge-and-trap GC-MS of polar and nonpolar organic compounds, *Chromatographia* 38 (1994) 709-714. <https://doi.org/10.1007/BF02269625>.
- [21] A.J. Boggess, T.L. White, M.A. Jones, T.B. Edwards, S.P. Harris, Development and comparison of purgeable mercury values in SRR samples measured by SRNL and Eurofins FGS, Report Number SRNL-STI-2019-00300 (2019). <https://doi.org/10.2172/1525793>.
- [22] B.B. Looney, T.L. White, T.B. Peters, A.J. Boggess, H.H. VerMeulen, E.D. Fabricatore, A.T. Brown, Mercury speciation using microcolumns with a direct mercury analyzer (DMA): development of analytical method for the Savannah River Site Liquid Waste System, Report Number SRNL-STI-2020-00148, Rev. 0 (2020). <https://doi.org/10.2172/1734662>.
- [23] US EPA, Estimation Program Interface (EPI) Suite™ v4.11 (Version 4.11), Washington DC, November 2012. <https://www.epa.gov/tsca-screening-tools/download-epi-suite-estimation-program-interface-v411>.
- [24] Senemasa, The Solubility of Elemental Mercury Vapor in Water, *Bull. Chem. Soc. Jpn*, 48 (1975) 1795-1798. <https://doi.org/10.1246/bcsj.48.1795>.

- [25] Senemasa, A. Masatake, D. Toshio, N. Hideo, Solubility Measurements of Benzene and the Alkylbenzenes in Water by Making Use of Solute Vapor, *Bull. Chem. Soc. Jpn*, 55 (1982) 1054-1062. <https://doi.org/10.1246/bcsj.55.1054>.
- [26] A.S. Kertes, H.L. Clever, M. Iwamoto, S.H. Johnson, H. Miyamoto, Solubility Data Series: Mercury in Liquids, Compressed Gases, Molten Salts and Other Elements, International Union of Pure and Applied Geochemistry, Analytical Chemistry Division Commission on Solubility Data, 29 (1987). <https://srdata.nist.gov/solubility/IUPAC/SDS-29/SDS-29.aspx>.
- [27] M.L. Huber, A. Laesecke, D.G. Friend, The vapor pressure of mercury, NISTIR 6643, National Institute of Standards and Technology Physical and Chemical Properties Division, Colorado (2006) 61. <https://dx.doi.org/10.6028/nist.ir.6643>.
- [28] Ambrose and C.H.S. Sprake, The vapour pressure of mercury, *J. Chem. Thermodyn.*, 4 (1972) 603-620. [https://doi.org/10.1016/0021-9614\(72\)90082-1](https://doi.org/10.1016/0021-9614(72)90082-1).
- [29] K.E. Gustafson, Molecular Diffusion Coefficients for Polycyclic Aromatic Hydrocarbons, Thesis Paper 1539617664, William & Mary, (1993) 87. <https://dx.doi.org/doi:10.25773/v5-pd77-fe86>.
- [30] P.G. Koster van Groos, B.K. Esser, R.W. Williams, J. R. Hunt, Isotope effect of mercury diffusion in air, *Environ. Sci. Technol.*, 48 (2014) 227–233. <https://doi.org/10.1021/es4033666>.
- [31] W.J. Massman, Molecular diffusivities of Hg vapor in air, O₂ and N₂ near STP and the kinematic viscosity and thermal diffusivity of air near STP, *Atmos. Environ.*, 33 (1999) 453-457. [https://doi.org/10.1016/S1352-2310\(98\)00204-0](https://doi.org/10.1016/S1352-2310(98)00204-0).
- [32] J. Kuss, J.O. Holzmann, R. Ludwig, An Elemental Mercury Diffusion Coefficient for Natural Waters Determined by Molecular Dynamics Simulation, *Environ. Sci. Technol.*, 43 (2009) 3183–3186. <https://doi.org/10.1021/es8034889>.
- [33] U.S. EPA, EPA On-line Tools for Site Assessment Calculation: Estimated Henry's Law Constants. <https://www3.epa.gov/ceampubl/learn2model/part-two/onsite/esthenry.html>, 2022 (accessed 26 March 2022).
- [34] J. Peng, A. Wan, Measurement of Henry's Constants of High-Volatility Organic Compounds Using a Headspace Autosampler, *Environ. Sci. Technol.*, 31 (1997) 2998-3003. <https://doi.org/10.1021/es970240n>.

Acknowledgements

This report is dedicated to Bill Wilmarth who was the SRNL lead for mercury research for many years before he recently passed. Bill encouraged breadth and diversity in the research of his collaborators.

Funding: Savannah River National Laboratory is operated by Battelle Savannah River Alliance for the U.S. Department of Energy under Contract No. 89303321CEM000080. This work was supported by the US Department of Energy Environmental Management Office of Technology Development under Contract Number DE-AC09-08SR2 and the US Department of Energy National Nuclear Security Administration in collaboration with Savannah River Remediation under Contract No. DE-AC09-09SR22505.

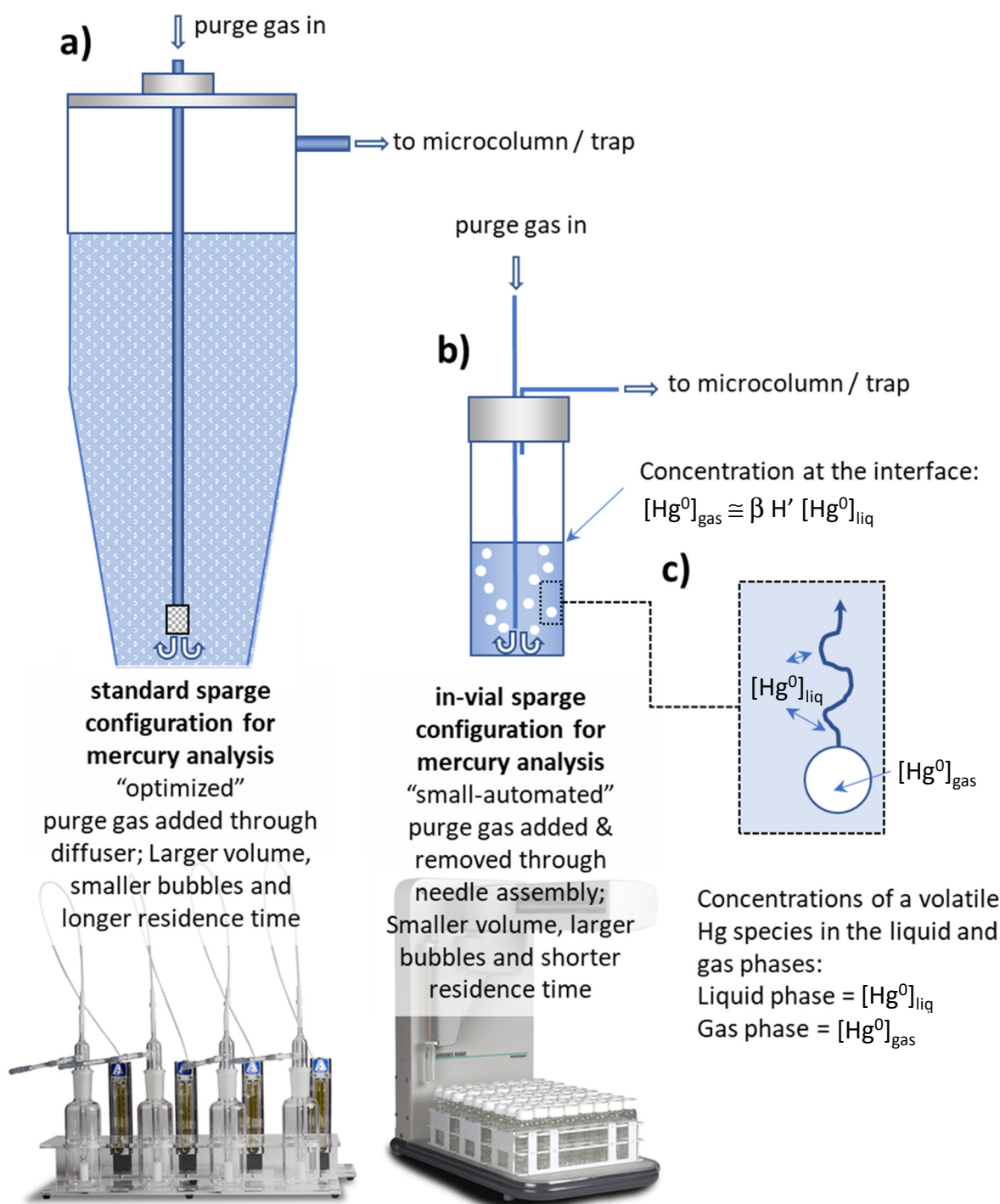
1 **Figure Captions:**

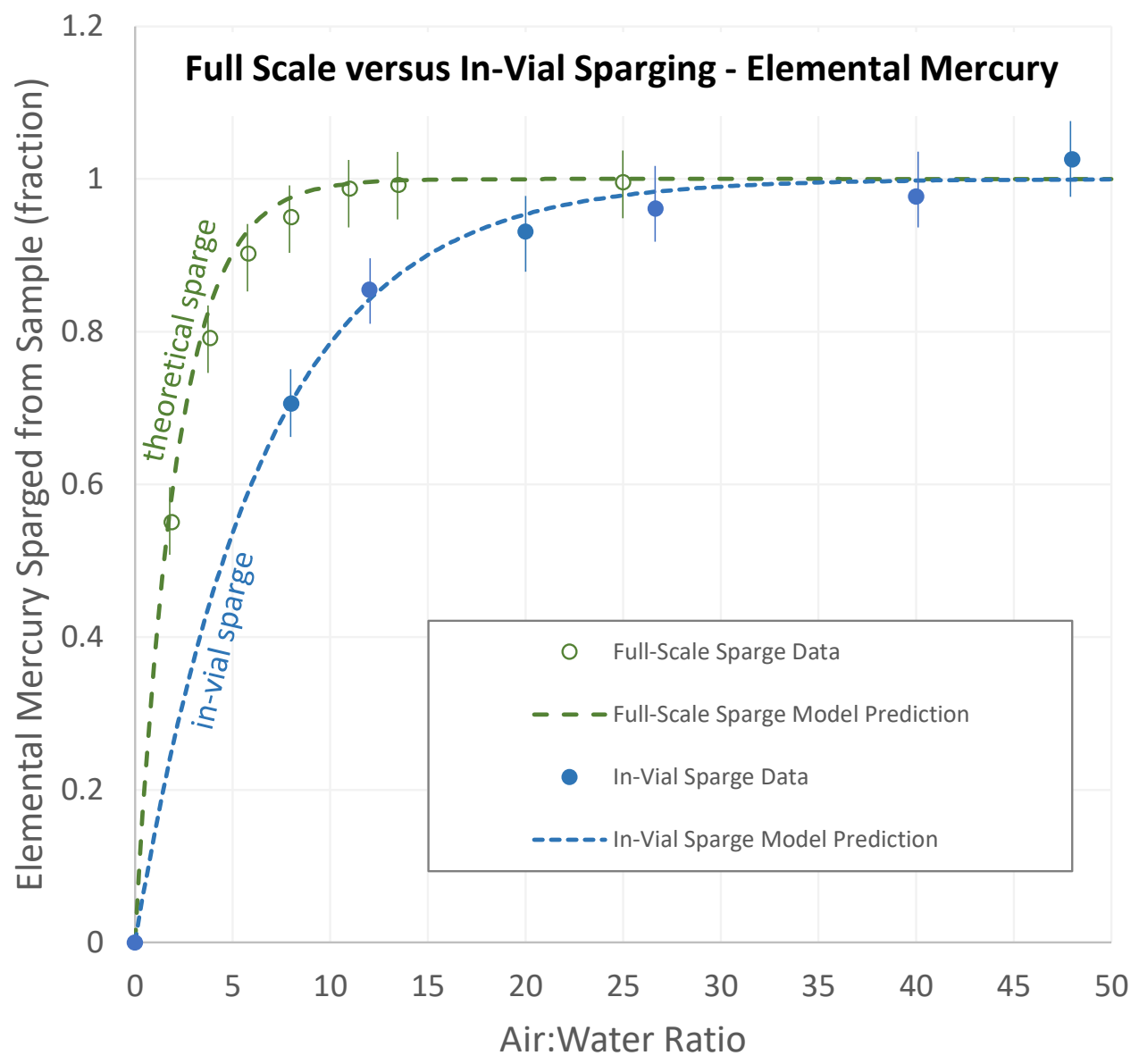
2 Figure 1. Schematic and Commercial Exemplars for: (a) Full-Scale Sparge System, (b) In-Vial Sparge
3 System, and (c) Conceptual Model and Mathematical Relationships used to Model Sparge Performance --
4 images adapted for figure courtesy of Brooks Rand Inc.

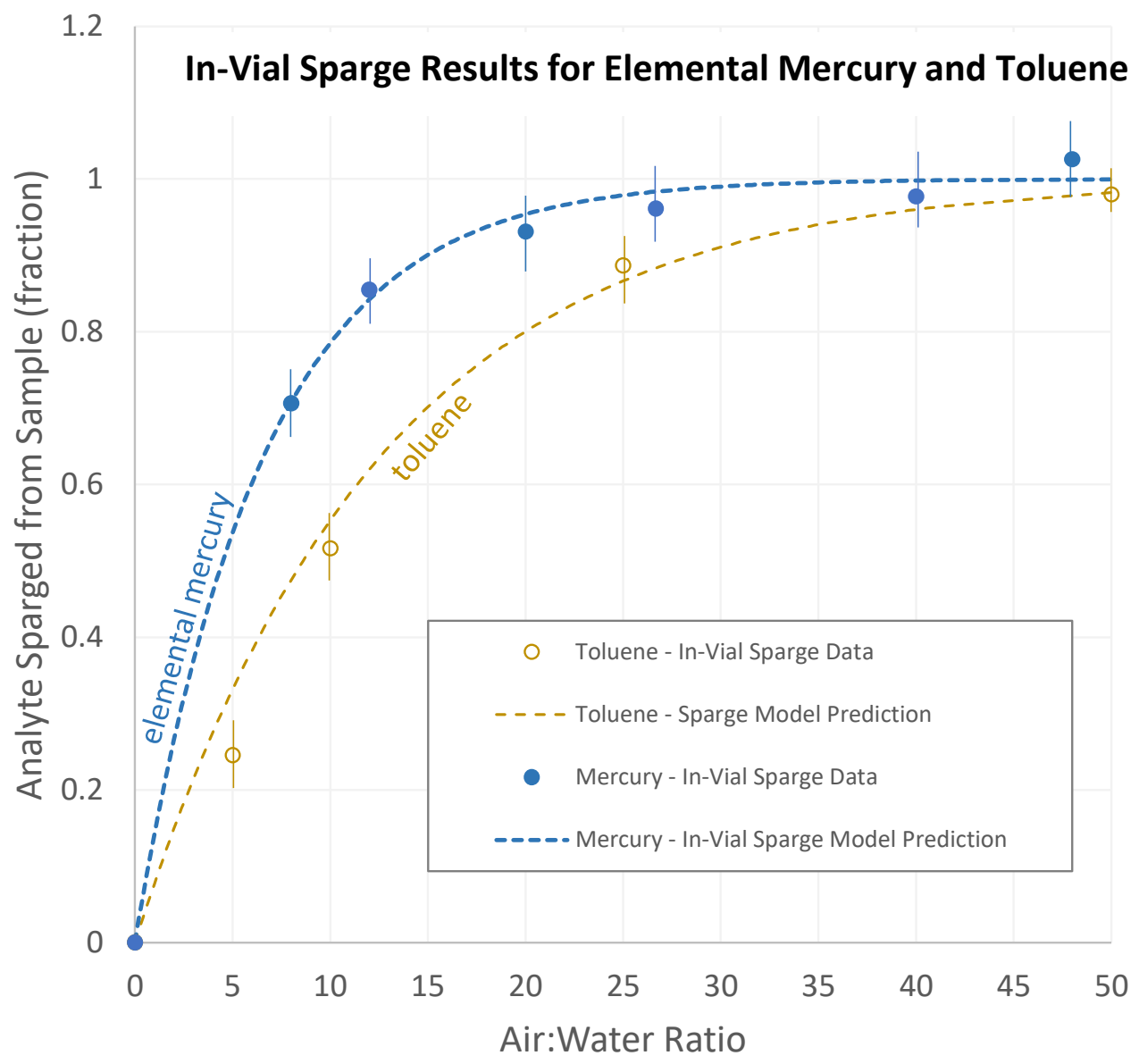
5 Figure 2. Elemental Mercury Sparging Data and Model Predictions for Full Scale and In-Vial Systems

6 Figure 3. Elemental Mercury and Toluene Data and Model Predictions for In-Vial System

7 Figure 4. Paired Bivariate Data Comparison -- Experimental Results and Model Predictions for all
8 Conditions and All Compounds







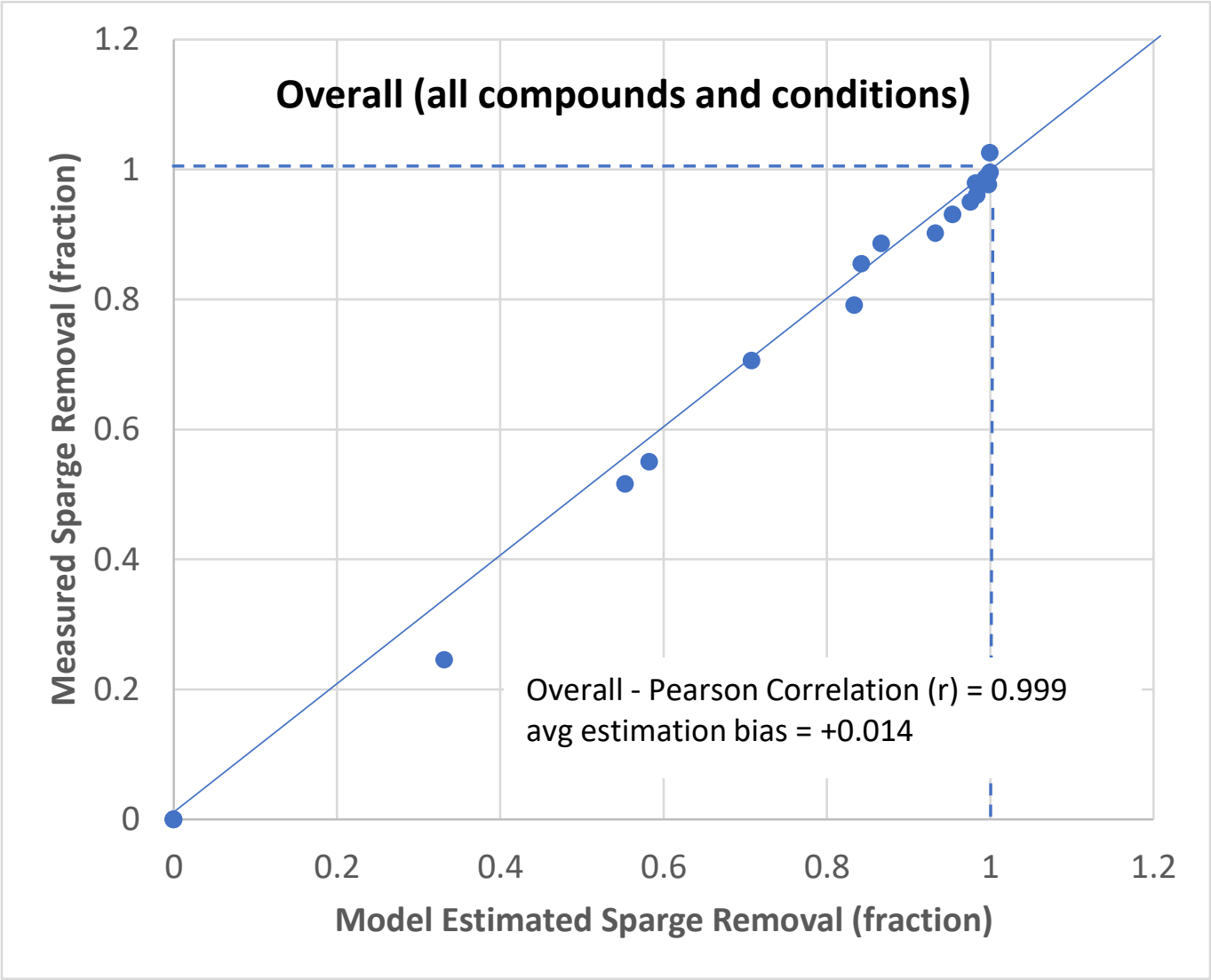



Table 1. Summary of Key Chemical and Physical Properties of Mercury and Toluene

| Parameter | Mercury (CAS No. 007439-97-6) | Toluene (CAS No. 000108-88-3) | References |
|---|----------------------------------|----------------------------------|----------------------|
| aqueous solubility (mg/L in water) ^a | 0.05 | 526 | [23, 24, 25, 26] |
| vapor pressure (mg/L in air) ^a | 0.020 | 128 | [23, 26, 27, 28] |
| diffusion coefficient in water (cm ² /sec) ^a | 19x10 ⁻⁶ | 9x10 ⁻⁶ | [29, 30, 34] |
| diffusion coefficient in air (cm ² /sec) ^a | 13x10 ⁻² | 7x10 ⁻² | [29, 30, 31] |
| octanol water partition coefficient (K _{ow}) | 4.16 | 537 | [23] |
| boiling point (°C) | 357 | 111 | [23, 27, 28] |
| melting point (°C) | -39 | -139 | [23] |
| Henry's Law air: water partition coefficient (dimensionless, H _{cc}) at 25 °C ^a | 0.466 | 0.244 | [23, 29, 30, 33, 34] |
| Henry's Law air: water partition coefficient (dimensionless, H _{cc}) at 20 °C ^b | 0.305 | 0.195 | [33] |
| ^a Tabulated values for reference solubility, vapor pressure, diffusion coefficients, and H _{cc} are for 25 °C | | | |
| ^b Tabulated H _{cc} representing ambient laboratory conditions (20 °C) used for modeling predictions | | | |

[Click here to view linked References](#)



Click here to access/download

Electronic Supplementary Material (online publication only)

Supplemental Information for j chrom v1.docx



1 **CRedit authorship contribution statement**

2 **Brian Looney:** Conceptualization, Methodology, Investigation, Formal analysis, Writing-Original Draft,
3 Writing-Reviewing & Editing; **Holly VerMeulen:** Writing-Original Draft, Data Interpretation, Writing-
4 Reviewing & Editing, Visualization; **Andrew Boggess:** Conceptualization, Investigation, Writing-
5 Reviewing & Editing.
6

Declaration of interests

☒ The authors declare that they have no known competing financial interests or personal relationships that could have appeared to influence the work reported in this paper.

☐ The authors declare the following financial interests/personal relationships which may be considered as potential competing interests: